The High lAtitude sNowfall Detection and Estimation aLgorithm for ATMS (HANDEL-ATMS): a New Algorithm for Snowfall Retrieval at High Latitudes

Andrea Camplani

Institute of Atmospheric Sciences and Climate - National Research Council - Rome, Italy

Co-Authors
Giulia Panegrossi (ISAC-CNR)
Paolo Sanò (ISAC-CNR)
Daniele Casella (ISAC-CNR)

EGU General Assembly 2023
Atmospheric Sciences
Precipitation: Measurement, Climatology, Remote Sensing, and Modelling

Supplementary Materials

Introduction

- ground-based measurements in regions where snowfall is predominant are scarce
  - use of satellite-based remote sensing measurements
- cloud/precipitation space-borne radars have limited spatial coverage
  - use of MW radiometer observations
- ambiguity and non-linearity of MW snowfall signature
  - development of snowfall retrieval algorithms based on machine learning (ML) methods

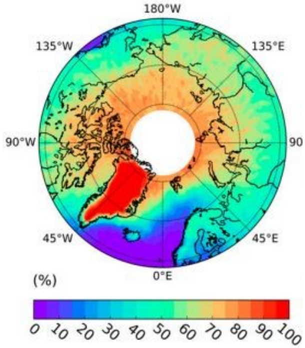

Figure: Frequency of snow profiles over all precipitating profiles over 2007–10. From: Edel, Leo, et al. "Arctic snowfall from CloudSat observations and reanalyses." https://doi.org/10.3390/rs11192200, 2020.

Motivations

- the **high-latitude regions** are the most challenging areas for snowfall retrieval
  - strong impact of the extremely variable background surface emissivity due to cold and dry atmosphere
  - influence of **supercooled water layer** on snowfall signature
- development of precipitation products for the European MetOp-SG mission at CNR-ISAC within the EUMETSAT HSAF program
  - Microwave Imager (MWI)
  - Microwave Sounder (MWS)

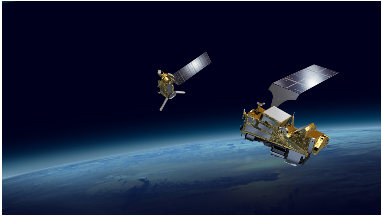

credit: EUMETSAT

High lAtitude sNow Detection and Estimation aLgorithm for ATMS (HANDEL-ATMS)

Innovative Aspects

- characterization of the background surface at the time of the overpass
- estimation of **multi-channel derived emissivity** for each observation
- comparison between the observed signal and a clear-sky simulated signal to highlight the snowfall signature
- **Machine Learning approaches**: Shallow Neural Networks, Self Organizing Maps (SOM), Linear Discriminant Analysis (LDA)

Limitations

- high-latitude environmental conditions (TPW < 10 mm, $T_{2m} < 280$ K)

Camplani, Andrea, et al. "The High lAtitude sNow Detection and Estimation aLgorithm for ATMS (HANDEL-ATMS): a new algorithm for the snowfall retrieval at the high latitudes." Submitted.

ATMS-CPR Coincidence Datasets

Period	2014-2016
Area	82°S-82°N 180°W-180°E
Total Observation Number	6.5 M
Snowfall Observation Number	1.1 M
Resolution (km)	15.8 x 15.8 (nadir) 30 x 68.4 (scan edge)
Input	**Source**
ATMS TB	NOAA
2 ATMS angle	
T2m	ECMWF
TPW	
freezing level	
Temperature, relative/specific humidity profiles	
Supercooled Water	DARDAR (liDAR+raDAR) Univ- Lille
Snow Water Path	2CSP-CPR
Surface Snowfall Rate	

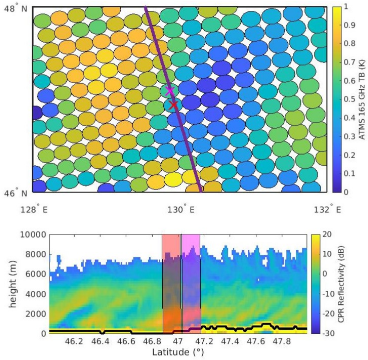

Surface Radiometric Characterization

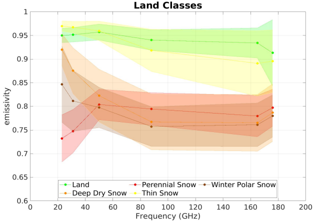

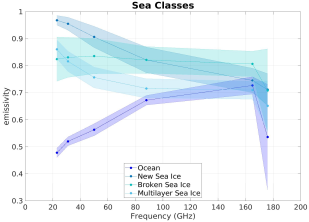

The Passive microwave Empirical cold Surface Classification Algorithm (PESCA)

- classification of the frozen background surface **at the time of the overpass**
- input: ATMS low-frequency channels (23 GHz, 31 GHz and 89 GHz) and environmental parameters
- three sea ice (New, Broken, Multilayer) and four snow-covered land classes (Perennial, Deep Dry, Thin, Winter Polar)
- **surface emissivity estimation** by appliyng a refinement process based on clustering approaches (SOM and LDA)

Camplani, Andrea, et al. ”The Passive microwave Empirical cold Surface Classification Algorithm (PESCA): Application to GMI and ATMS.” https://doi.org/10.1175/JHM-D-20-0260.1, 2021.

PESCA Design

SEA ICE

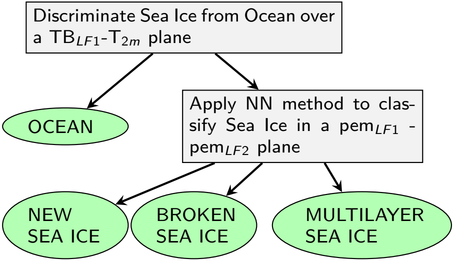

SNOW COVER

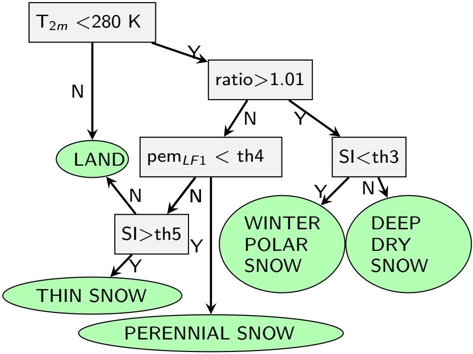

ratio	$\frac{TB_{23QV}}{TB_{31QV}}$
SI	TB_{23QV}-TB_{89QV}
pem_{LFi}	$\frac{TB_{LFi}}{T_{2m}}$
TB_{LF1}	TB_{23QV}
TB_{LF2}	TB_{31QV}
th_3	257 K -T_{2m}
th_4	$\frac{465K - T_{2m}}{225K}$
th_5	$\frac{3K}{\cos\theta}$

Refinement Process

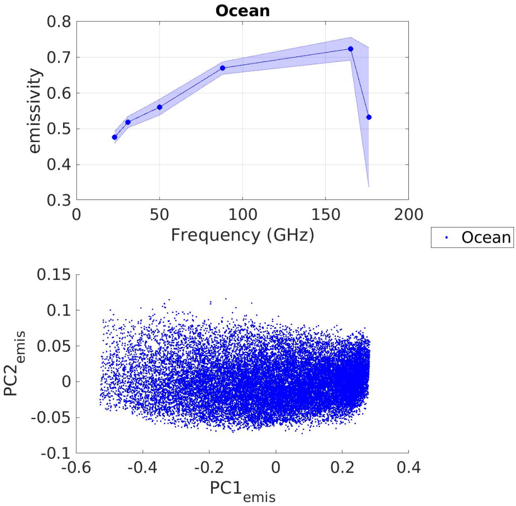

Estimate emissivity spectra by considering clear-sky observations

Figure: Ocean Class - Refinement Process - 2 Clusters

Refinement Process

Estimate emissivity spectra by considering clear-sky observations

↓

Apply unsupervised classification model (SOM) to reduce inner variability

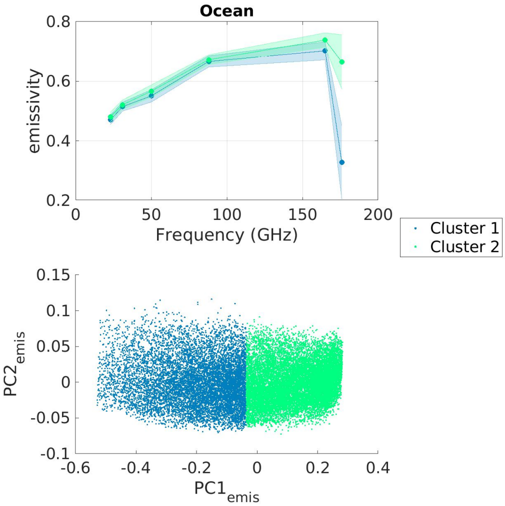

Figure: Ocean Class - Refinement Process - 2 Clusters

Refinement Process

Estimate emissivity spectra by considering clear-sky observations

↓

Apply unsupervised classification model (SOM) to reduce inner variability

↓

Apply supervised classification model (LDA) to rebuild the previous classification by using PESCA variables

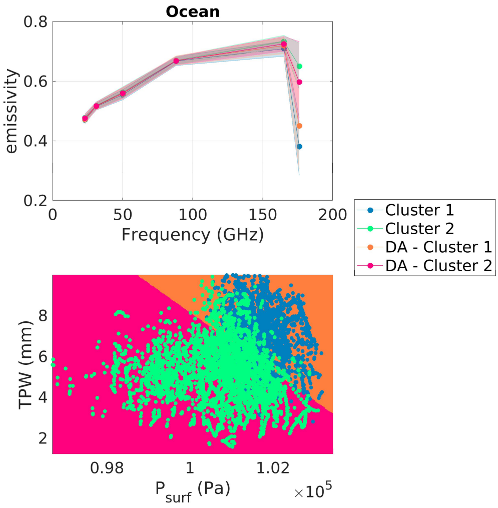

Figure: Ocean Class - Refinement Process - 2 Clusters

Refinement Process

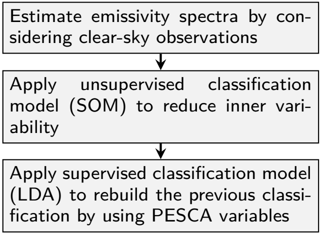

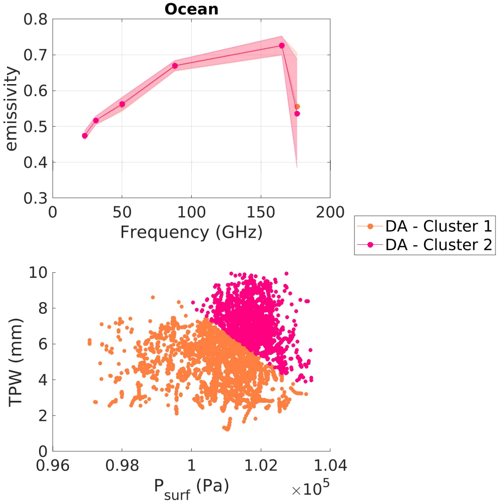

Figure: Ocean Class - Refinement Process - 2 Clusters

Refinement Process

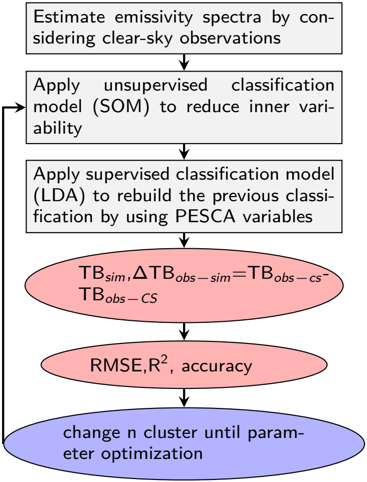

Class	Ocean			
Predictors	P_{surf},TPW,T_{2m}			
	input	SOM	DA training	DA test
RMSE	7.7	3.2	3.3	3.6
accuracy			0.9	0.85
R^2		0.92	0.81	0.78

Comparison between TB_{obs} and Clear Sky TB_{sim}

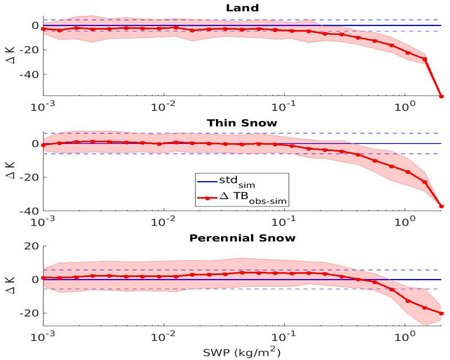

165.5 GHz $\Delta TB_{obs-sim}$ as a function of SWP

- blue belt: standard deviation of TB_{sim}
- red belt: mean and standard deviation of $\Delta TB_{obs-sim}$
- Δ K $> 0 \hookrightarrow TB_{obs} > TB_{sim}$ emission effect
- Δ K $< 0 \hookrightarrow TB_{obs} < TB_{sim}$ scattering effect

Snowfall signature dependence on background surface class:

- Land: scattering for SWP $> 0.1\ \frac{kg}{m^2}$; for SWP $< 0.1\ \frac{kg}{m^2}$ Δ K < 0
- Perennial Snow: scattering for SWP$> 0.5\ \frac{kg}{m^2}$, for SWP $< 0.1\ \frac{kg}{m^2}$ Δ K > 0
- Thin Snow: scattering SWP$> 0.3\ \frac{kg}{m^2}$, for SWP $< 0.3\ \frac{kg}{m^2}$ Δ K ≈ 0

Snowfall Retrieval Modules - Input Selection

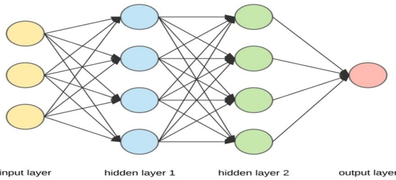

$n_{neurons}$=$n_{predictors}$ hyperbolic tangent

$n_{neurons}$=60 hyperbolic tangent

$n_{neurons}$=30 logarithmic tangent

$n_{neurons}$=30 linear transfer

SSRD performances	POD	FAR	HSS
$\Delta TB_{obs-sim}$	0.75	0.29	0.48
TB	0.81	0.18	0.65
TB & env par	0.82	0.17	0.67
TB & $\Delta TB_{obs-sim}$	0.84	0.16	0.68

Modules

- SWP detection (SWPD)
- SWP estimation (SWPE)
- SSR detection (SSRD)
- SSR estimation (SSRE)

- TB_{sim}=f (ϵ*,env par)
- $\Delta TB_{obs-sim}$=TB_{obs}-TB_{sim}

HANDEL-ATMS Flowchart

Date	Orbit		Time UTC	
	CPR	ATMS	CPR	ATMS
2015 11/24	50937	21117	20;45:02 20:53:45	20:42:09 20:51:02

Apply PESCA to ATMS overpass

↓

Apply ML methods to identify emissivity specra

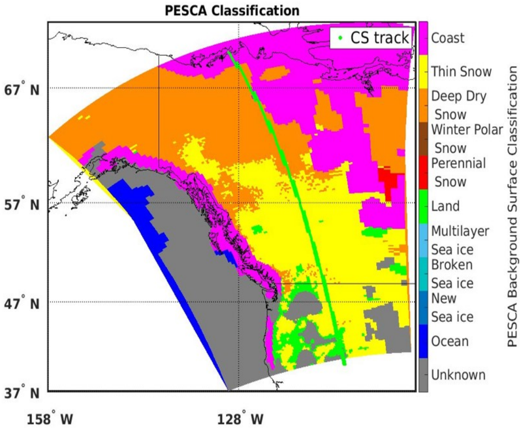

HANDEL-ATMS Flowchart

Date	Orbit		Time UTC	
	CPR	ATMS	CPR	ATMS
2015 11/24	50937	21117	20;45:02 20:53:45	20:42:09 20:51:02

Apply PESCA to ATMS overpass

↓

Apply ML methods to identify emissivity specra

↓

Estimate TB_{sim}

↓

Calculate $\Delta TB_{obs-sim}$

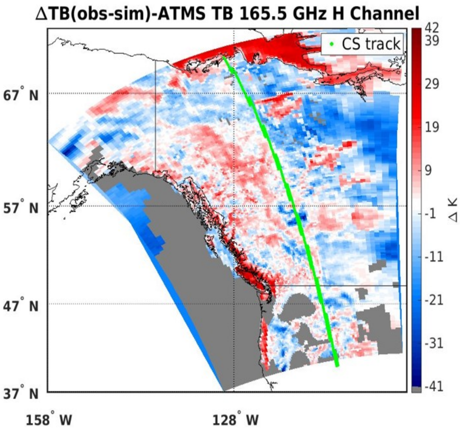

HANDEL-ATMS Flowchart

Date	Orbit		Time UTC	
	CPR	ATMS	CPR	ATMS
2015 11/24	50937	21117	20;45:02 20:53:45	20:42:09 20:51:02

Apply PESCA to ATMS overpass

↓

Apply ML methods to identify emissivity specra

↓

Estimate TB_{sim}

↓

Calculate $\Delta TB_{obs-sim}$

↓

$\Delta TB_{obs-sim}$, TBs, DEM, scan angle, PESCA flag

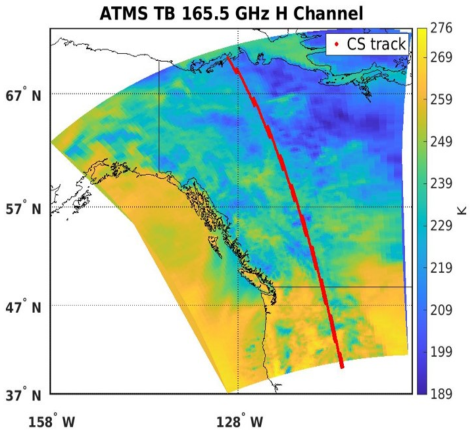

HANDEL-ATMS Flowchart

Date	Orbit		Time UTC	
	CPR	ATMS	CPR	ATMS
2015 11/24	50937	21117	20;45:02 20:53:45	20:42:09 20:51:02

Apply PESCA to ATMS overpass

↓

Apply ML methods to identify emissivity specra

↓

Estimate TB_{sim}

↓

Calculate $\Delta TB_{obs-sim}$

↓

$\Delta TB_{obs-sim}$, TBs, DEM, scan angle, PESCA flag

↓

SWPD module-SWPE module

HANDEL-ATMS Snow Water Path Detection

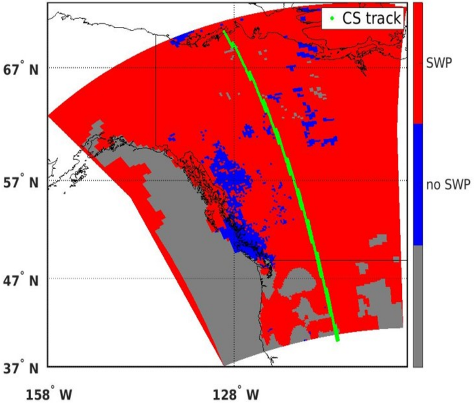

HANDEL-ATMS Flowchart

Date	Orbit		Time UTC	
	CPR	ATMS	CPR	ATMS
2015 11/24	50937	21117	20;45:02 20:53:45	20:42:09 20:51:02

Apply PESCA to ATMS overpass

↓

Apply ML methods to identify emissivity specra

↓

Estimate TB_{sim}

↓

Calculate $\Delta TB_{obs-sim}$

↓

$\Delta TB_{obs-sim}$, TBs, DEM, scan angle, PESCA flag

↙ ↘

SWPD module-SWPE module

SSRD module-SSRE module

HANDEL-ATMS Surface Snowfall Rate Detection

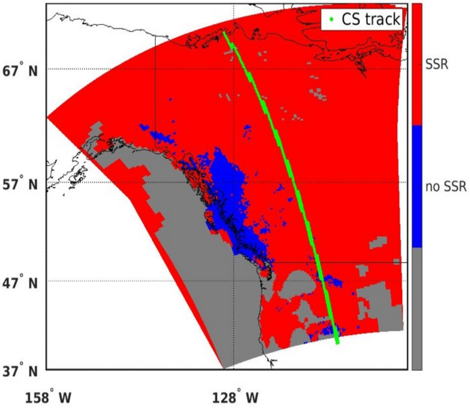

HANDEL-ATMS Flowchart

Date	Orbit		Time UTC	
	CPR	ATMS	CPR	ATMS
2015 11/24	50937	21117	20;45:02 20:53:45	20:42:09 20:51:02

Apply PESCA to ATMS overpass

↓

Apply ML methods to identify emissivity specra

↓

Estimate TB_{sim}

↓

Calculate $\Delta TB_{obs-sim}$

↓

$\Delta TB_{obs-sim}$, TBs, DEM, scan angle, PESCA flag

↙ ↘

SWPD module-SWPE module | SSRD module-SSRE module

↓ (from SWPD module-SWPE module)

Apply SWP mask over SWP estimation

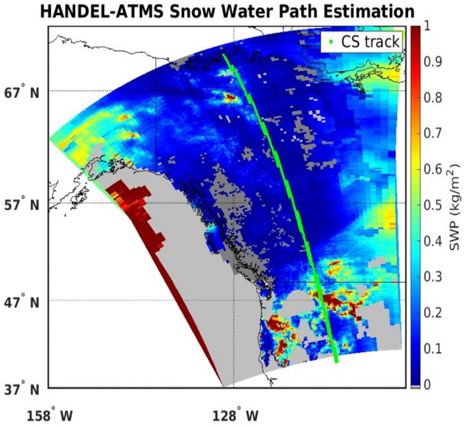

HANDEL-ATMS Flowchart

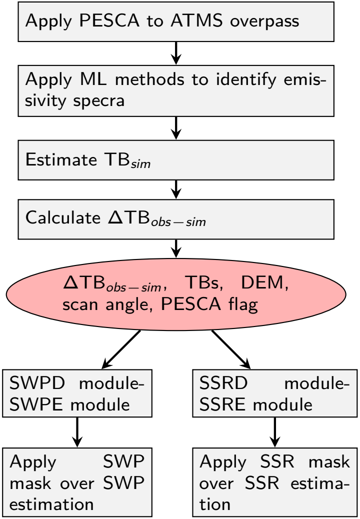

Date	Orbit		Time UTC	
	CPR	ATMS	CPR	ATMS
2015 11/24	50937	21117	20;45:02 20:53:45	20:42:09 20:51:02

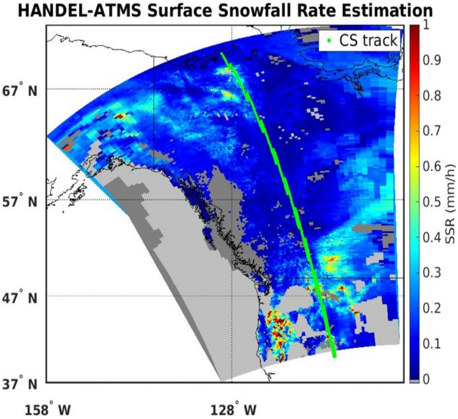

HANDEL-ATMS Detection Performances

	POD	FAR	HSS
SWP	0.85	0.15	0.70
SSR	0.84	0.16	0.69

DEPENDENCE ON HUMIDITY

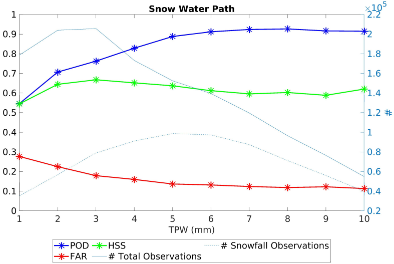

DEPENDENCE ON TEMPERATURE

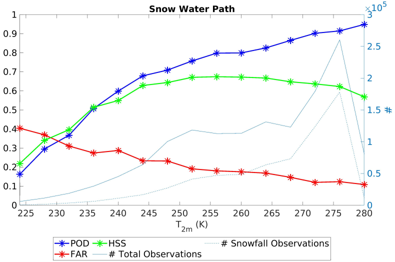

HANDEL-ATMS Estimation Performances

	RMSE	bias	R^2 (-)
SWP ($\frac{kg}{m^2}$)	0.047	0.001	0.72
SSR ($\frac{mm}{h}$)	0.079	0.002	0.61

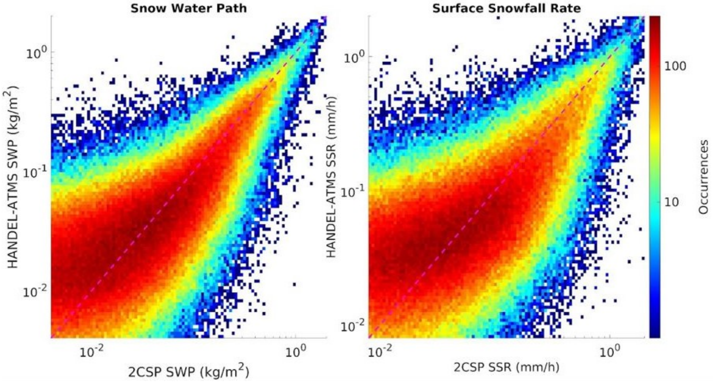

SLALOM-CT VS HANDEL-ATMS

SLALOM-CT

- snowfall retrieval on a global scale
- ATMS TBs, PESCA output, model-derived parameters

HANDEL-ATMS

- high-latitude conditions
- ATMS TBs, $\Delta TB_{obs-sim}$, PESCA output

	POD		FAR	
	SLALOM CT	HANDEL ATMS	SLALOM CT	HANDEL ATMS
T_{2m}<280 K TPW<10 mm	0.82	0.84	0.19	0.16
T_{2m}<250 K TPW<5 mm	0.64	0.68	0.27	0.23
T_{2m}<240 K TPW<3 mm	0.45	0.54	0.33	0.28

Sanò, Paolo, et al. "A Machine Learning Snowfall Retrieval Algorithm for ATMS." Remote Sensing 14.6 (2022): 1467.

SLALOM-CT Flowchart

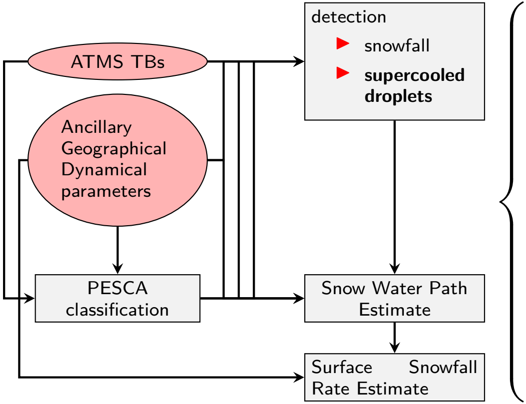

PIXEL BASED METHODS

- Random Forest (RF)
- Gradient/Adaptive Boosting (GB,Ada)
- Shallow Neural Networks (S-NNA)

IMAGE BASED METHODS

- Convolutional Neural Networks (VGG, ResNet)

Arctic - 2015/01/03

Date	CPR Orbit	ATMS Orbit	CPR Time UTC	ATMS Time UTC
2015/01/03	46196	16498	07:28:29-07:30:11	07:21:24-07:23:08

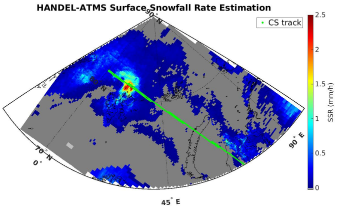

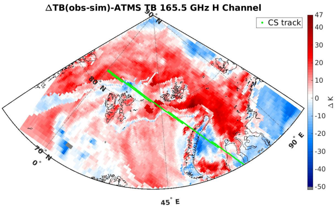

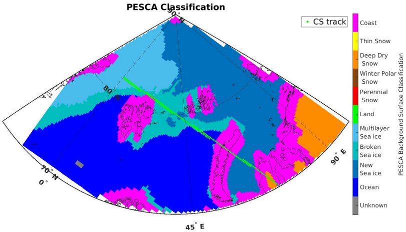

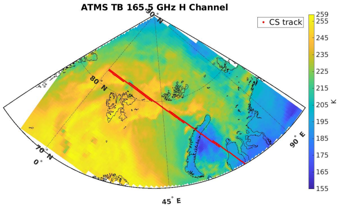

Arctic - 2015/01/03 - CloudSat Track

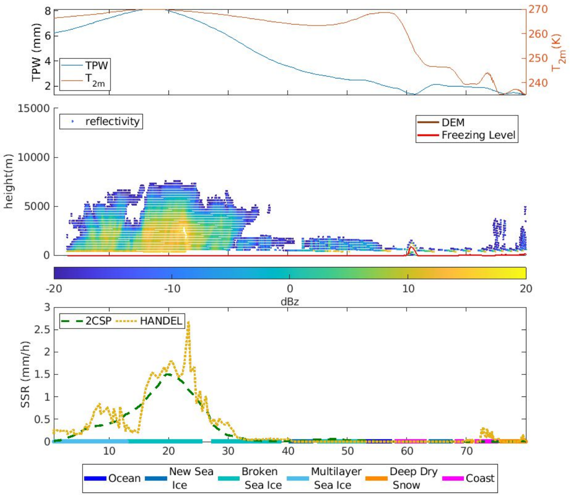

Future Perspectives

- development of a module for **supercooled water layer detection**, to be integrated into HANDEL-ATMS
- application of **deep-learning techniques**
- integration between **HANDEL-ATMS** and **SLALOM-CT** approach in order to optimize the global snowfall application for the high-latitudes regions
- development of precipitation products for the **MetOp-SG mission** at CNR-ISAC within the **EUMETSAT HSAF program**
  - Microwave Imager (MWI)
  - Microwave Sounder (MWS)
- contribution to the **ESA RainCast study** carried out at CNR-ISAC dedicated to the assessment of snowfall observation capabilities of the future spaceborne MW passive sensors (**Arctic Weather Satellite**, **AWS**)

Thanks for your kind attention

References

- Casella, D., Panegrossi, G., Sanò, P., Marra, A. C., Dietrich, S., Johnson, B. T., Kulie, M. S., Evaluation of the GPM-DPR snowfall detection capability: Comparison with CloudSat-CPR. Atmospheric Research, 197, 64-75, https://doi.org/10.1016/j.atmosres.2017.06.018, 2017.
- Panegrossi, G., Rysman, J. F., Casella, D., Marra, A. C., Sanò, P., Kulie, M. S., CloudSat-based assessment of GPM Microwave Imager snowfall observation capabilities. Remote Sensing, 9(12), 1263, https://doi.org/10.3390/rs9121263, 2017.
- Rysman, J. F., Panegrossi, G., Sanò, P., Marra, A. C., Dietrich, S., Milani, L., Kulie, M. S., SLALOM: An all-surface snow water path retrieval algorithm for the GPM Microwave Imager. Remote Sensing, 10(8), 1278, https://doi.org/10.3390/rs10081278, 2018.
- Rysman, J. F., Panegrossi, G., Sanò, P., Marra, A. C., Dietrich, S., Milani, L., Kulie, M. S., Casella, D., Camplani, A., Claud, C. Edel, L.: Retrieving surface snowfall with the GPM Microwave Imager: A new module for the SLALOM algorithm, Geophysical Research Letters, 46(22), 13593-13601, https://doi.org/10.1029/2019GL084576, 2019.
- Panegrossi, G., Casella, D., Sanò, P., Camplani, A., Battaglia, A, Recent advances and challenges in satellite-based snowfall detection and estimation, In Precipitation Science (pp. 333-376), Elsevier, https://doi.org/10.1016/B978-0-12-822973-6.00015-9, 2022.
- Camplani, A., Casella, D., Sanò, P., Panegrossi, G.: The Passive Microwave Empirical Cold Surface Classification Algorithm (PESCA): Application to GMI and ATMS, Journal of Hydrometeorology, vol. 22, no. 7. https://doi.org/10.1175/JHM-D-20-0260.1, 2021.
- Sanò, P., Casella, D., Camplani, A., D'Adderio, L. P., Panegrossi, G., A Machine Learning Snowfall Retrieval Algorithm for ATMS, Remote Sensing, 14(6), 1467. https://doi.org/10.3390/rs14061467, 2022.

Andrea.Camplani@artov.isac.cnr.it